Floating particle trapping and diffusion in vegetated open channel flow

Andrea Defina[1] and Paolo Peruzzo[1]

Received 23 March 2010; revised 5 July 2010; accepted 19 August 2010; published 13 November 2010.

[1] In this paper we present early results of laboratory experiments to investigate the transport and diffusion of floating particles (e.g., buoyant seeds) in open channel flow with emergent vegetation. The experiments are aimed at providing a better understanding of the relevant particle-vegetation interaction mechanisms responsible for the observed diffusion processes. Qualitative observational data are then used to set up a stochastic model for floating particle transport and diffusion. Quantitative observations, such as the distribution of distances travelled by a particle before it is permanently captured by a plant and the arrival-time distributions at prescribed cross sections along the vegetated test section, are instead used to calibrate and validate the model. The comparison between theoretical predictions and experimental results is quite satisfactory and suggests that the observed relevant aspects of the particle-vegetation interaction processes are properly described in the model.

Citation: Defina, A., and P. Peruzzo (2010), Floating particle trapping and diffusion in vegetated open channel flow, *Water Resour. Res.*, *46*, W11525, doi:10.1029/2010WR009353.

1. Introduction

[2] Hydrochory, or dispersal of disseminules by water, plays a central role in the structuring of the riparian community [e.g., *Andersson et al.*, 2000; *Rand*, 2000; *Merritt and Wohl*, 2002; *Riis and Sand-Jensen*, 2006]. Focusing on seed dispersal, we distinguish floating from nonfloating seeds.

[3] Nonfloating seeds behave approximately as suspended sediment or neutrally buoyant particles. In this case, field studies agrees in indicating that the flow velocity is the main factor influencing seed dispersal and deposition [*Andersson et al.*, 2000; *Merritt and Wohl*, 2002]. In addition, experimental investigations performed both in situ and in the laboratory provided details of the diffusion processes in the presence of vegetation [*Lopez and Garcia*, 1998; *Nepf*, 1999; *White and Nepf*, 2003; *Lightbody and Nepf*, 2006; *Sharpe and James*, 2006; *Murphy et al.*, 2007; *Nepf et al.*, 2007] and studied the details of particle trapping mechanisms [*Palmer et al.*, 2004].

[4] The behavior of floating particles differs substantially from that of suspended sediment as the particles are affected by hydrodynamic phenomena that develop at the free surface (e.g., wind drag and surface tension effects). To date, the importance of floating ability in the dispersal of seeds has not been assessed in great detail. Field studies, which mainly focused on seed dispersal in rivers, have shown that seed buoyancy enhances aquatic seed dispersal [*Nilsson and Danvind*, 1997; *Van den Broek et al.*, 2005]. As such, the key factor in the floating seed dispersal is usually considered to be the potential duration of buoyancy, which has received much interest [*Van den Broek et al.*, 2005].

[5] Floating seed dispersal also occurs in tidal estuaries and coastal lagoons [e.g., *Huiskes et al.*, 1995; *Rand*, 2000; *Riis and Sand-Jensen*, 2006]. In fact, many salt-marsh species appear to be adapted to dispersal by water, as their diaspores such as seeds are able to float for some time in seawater [*Wolters et al.*, 2008]. Despite the difficulty of studying floating seed dispersal in situ, few studies have addressed this issue through laboratory experiments. *Merritt and Wohl* [2002] studied the influence of the hydrologic regime, specifically channel morphology and dispersion phenology on seed deposition patterns in a laboratory channel with fluvial features such as flow expansions and constrictions, pools, point bars, islands, and slackwater areas. However, the complex channel morphology used in the experiments makes it difficult to identify the fundamental mechanisms responsible for the observed behaviours.

[6] Laboratory experiments were performed with five different buoyant seeds (www.interscience.wiley.com, DOI: 10.1002/rra.1093). An array of vertical cylinders was used to mimic an emergent plant canopy and it was found that the main trapping mechanism was through the Cheerios effect, whereby floating particles are attracted toward plant leaves by the rising meniscus. The trapping frequency increased with increasing stem density and with decreasing particle mass (i.e., particle inertia). It was also observed that, unlike suspended sediment or neutrally buoyant tracer, floating particles were not often trapped in the wake region behind the cylinders.

[7] All these studies give valuable insight into floating particle transport, diffusion, and trapping in the presence of emergent vegetation. However, they are not extensive enough to give a complete and detailed picture of the complex processes that govern floating particle dispersal, and there is a clear need for further research.

[8] The purpose of our investigation is to improve our understanding of floating particle diffusion processes, focusing on particle trapping mechanisms by emergent vegetation,

[1]Dipartimento di Ingegneria Idraulica, Marittima Ambientale e Geotecnica, Università di Padova, Padua, Italy.

0043-1397/10/2010WR009353

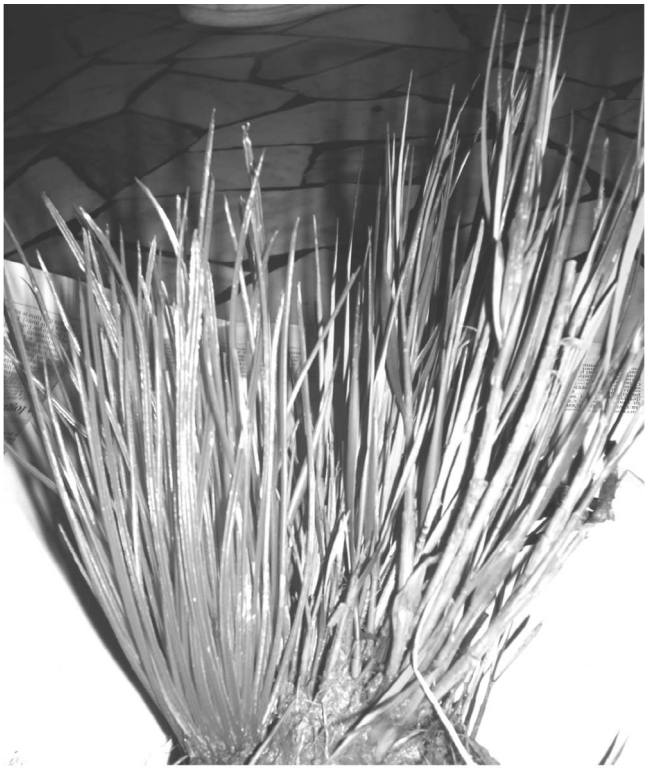

Figure 1. Plastic plant used in the experiments (left) compared to young *SpartinaMaritima* collected in the lagoon of Venice (Italy) (right).

through controlled laboratory experiments (section 2.1). The experimental findings are then used to set up a model to predict floating particle dispersal (section 2.2). Section 3 is devoted to a comparison between model predictions and experimental results. Concluding remarks are then given in section 4.

2. Materials and Methods

[9] In this study, we use laboratory experiments to explore the details of the processes that control floating particle transport and diffusion in the presence of emergent vegetation. This work has been motivated by the problem of studying the spreading of floating seeds transported by tidal flow over salt marshes, encroached with halophytic vegetation, in the lagoon of Venice (Italy). Therefore the investigated experimental conditions (e.g, flow velocity, water depth, plant morphology, and density) are similar to those commonly found in this estuarine environment.

[10] Observational data are used to set up a stochastic model which includes the relevant aspects of particle-vegetation interaction process. We then use quantitative observations, such as the distribution of distances travelled by a particle before it is permanently captured by a plant and the arrival-time distributions at prescribed cross sections along the vegetated test section, to calibrate and validate the model.

2.1. Experiments

[11] The experiments are carried out in a 6 m long, 0.3 m wide tilting flume. Water is recirculated through the channel via a constant head tank that maintains steady flow conditions. A magnetic flowmeter accurately measures the flow rate: A steady discharge of 2 l/s is introduced in the flume in all the experiments. Bed slope and a downstream weir are adjusted to achieve uniform flow conditions with a water depth of 0.1 ± 0.002 m resulting in a bulk velocity of 0.066 m/s. The model plant canopy consists of plastic plants inserted into a 3.0 m long, perforated Plexiglas board that covers the middle part of the flume. The plastic plants, which resemble *SpartinaMaritima* (Figure 1), are 0.15 m high and are composed of approximately 120 leaves. Leaves have an elliptical section with the major diameter $d \approx 2$ mm and the ratio of minor to major axes of ≈0.7. Two vegetation configurations are studied and are referred to as *staggered* and *random* in the text (see Figure 2). The staggered configuration has a density $n_p = 85$ plants/m^2, the random configuration has a density $n_p = 56$ plants/m^2.

[12] To achieve uniform flow across the test section bed slope is $s_b = 0.0034$ for the staggered configuration and $s_b = 0.0025$ for the random configuration. Two different particles are used in the experiments to mimic buoyant seeds: particle A is an irregularly shaped wood particle that can be described approximately as a sphere having a diameter of 2.5 mm and a relative density of 0.95. Particle B is a smooth spherical berry with a diameter of 3.7 mm and a relative density of 0.83.

[13] Some preliminary investigations used lighter particles such as expanded polystyrene (EPS) with a relative density of 0.03. However, very light particles are extremely susceptible to trapping and all the particles released just upstream of the test section were permanently captured by the vegetation after travelling a short distance (shorter than 0.5 m for EPS particles). This behavior prevents us from performing a statistically reliable study of particle dispersal.

[14] In addition, we specify that this study focuses on longitudinal characteristics of floating particle dispersion, in fact the flume is relatively narrow and this does not allow

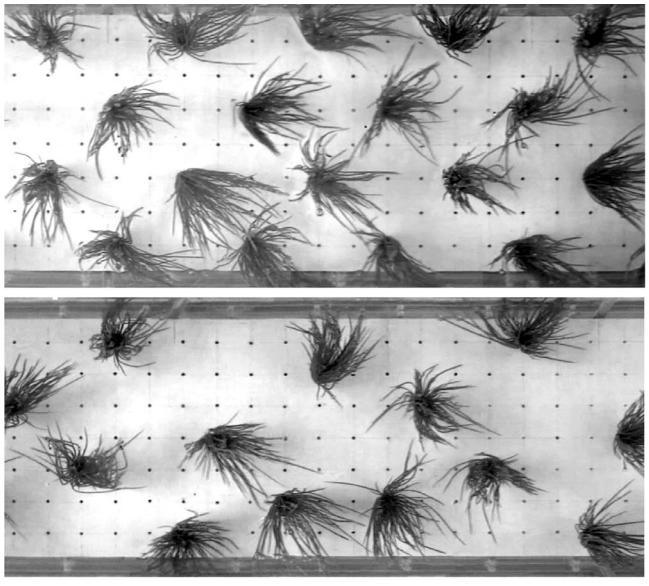

Figure 2. Vegetation configurations used in the experiments with notation. The upper panel shows the staggered configuration, the lower panel shows the random configuration. Spacing between *dots* on the flume bed is 4 cm; flow is from left to right.

Table 1. Summary of Experimental Results and Model Parameters Calibration[a]

	Staggered Particle A	Random Particle A	Staggered Particle B
$\Delta S(m)$	0.108	0.108	0.108
λ(m)	1.26	1.55	0.53
$\lambda/\Delta S$	11.7	11.5	4.9
$P_i P_c$	0.082	0.083	0.184
P_i	0.295	0.295	0.360
P_c	*0.278*	*0.281*	*0.511*
P_i/P_c	*1.06*	*1.05*	*0.704*
$P_i(1-P_c)$	*0.213*	*0.212*	*0.176*
P_L	0.105	0.105	0.105
T_S(s)	1.7	1.7	2.7
T_L(s)	55.0	55.0	80.0
U_0(m/s)	0.073	0.081	0.073

[a]Numbers in italics indicate relevant probability values computed using the nonitalicized calibrated model parameters values.

for a meaningful study of the transverse diffusion. The relatively narrow channel width can also affect the longitudinal particle propagation; however, vegetation is likely to reduce the effects of lateral confinement by promoting a more uniform average velocity in the transverse direction.

[15] Experimental observations are performed from both the Lagrangian and the Eulerian points of view. Within the Lagrangian framework we release one single particle at a time just upstream of the test section and we observe the particle path and behavior. We also measure the distance travelled by the particle before it is permanently captured by a plant (we assume a particle is permanently captured if it stays attached to one plant for more than 10 min, i.e., a time interval that is longer by more than one order of magnitude than the mean time a particle takes to travel the whole test section).

[16] For each vegetation configuration and particle type, approximately 400 particles are released and monitored to qualitatively observe the processes they experience and quantitatively evaluate the distance they travel before being permanently captured (see Table 1). A few particle paths are also recorded with a camera mounted on a moving carriage, supported by a pair of rails along the flume, and driven by hand. Recorded frames (frame rate is 12.5 Hz) are then extracted and analyzed to track particle trajectory and to determine particle velocity. Accuracy in reconstructing instantaneous particle position is rather rough (particle position is determined with an error of ±1 mm); however, results give a reliable picture of particle path characteristics.

[17] An example of the recorded particle trajectory is shown in Figure 3, where we observe that the particle path is significantly affected by the heterogeneity of the velocity field induced by the vegetation. We observe eight interaction events, indicated with an arrow, where the particle is slowed down and its velocity reduces to zero for a very short time (less than 0.1 s). At $x \approx 0.25$ m the particle enters the wake region behind a group of densely arranged leaves and it experiences an irregular motion with negative velocities; this wake trapping lasts approximately 1 s.

[18] Figure 4 shows the probability density function (pdf) of particle longitudinal velocity computed from the recorded particle trajectories: the pdf is biased toward the smaller velocities, indicating that the diffusion process is controlled not only by temporal and spatial heterogeneity of the surface velocity field but also by the delay due to particle slowdown and/or short-time trapping.

[19] Within the Eulerian framework, groups of 50 particles are released at one moment uniformly distributed along a cross section just upstream of the test section and the passage of particles at fixed cross sections along the test section is recorded with a camera. Recording sections are located at the distances of 1.0, 2.0, and 3.0 m for particle A and 0.5, 1.0, 1.5, and 2.0 m for particle B from the upstream end of the test section. Eight groups with 50 particles are released for each vegetation configuration, particle type, and recording section. From the video analysis we determine the number of particles that pass the recording cross sections and we measure the time required by each particle to reach these sections (Figure 5). It is worth noting, in Figure 5, that scaling the distances X of the recording cross sections by the length scale $1/\sqrt{n_p}$, n_p being the number of plants per unit area, makes the mean arrival times for particle A to collapse onto a single line regardless the vegetation configuration.

[20] Direct observation and video analysis also allows us to recognize the relevant aspects of the interaction between floating particles and vegetation and the mechanisms responsible for the temporary and the permanent trapping of particles by plants. When a particle interacts with a plant it is slowed down by three primary mechanisms: surface tension attraction through the Cheerios effect, inertial impaction, and wake trapping.

[21] The Cheerios effect [e.g., *Vella and Mahadeven*, 2005] is the tendency for floating particles to be attracted toward a leaf by the rising meniscus: If a particle approaches a leaf within a distance comparable to the leaf diameter, then

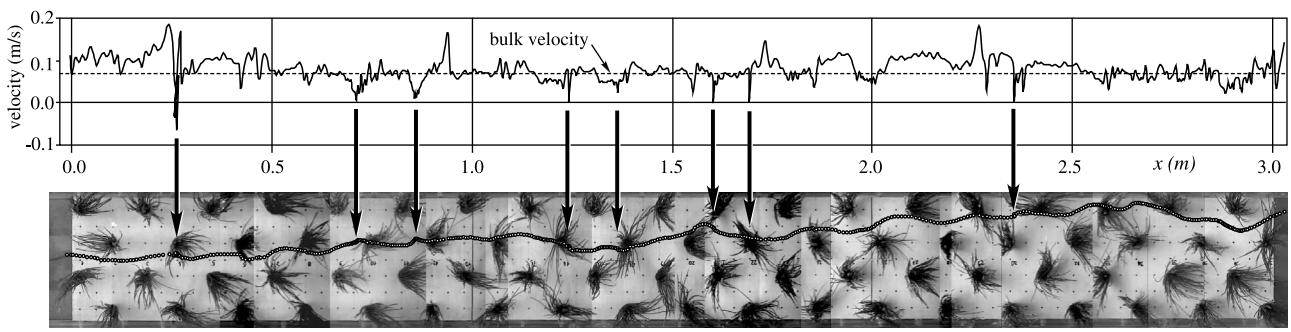

Figure 3. Particle longitudinal velocity as a function of the distance along the test section (upper panel), and plan view of the test section with the indication of the particle path (lower panel). Arrows denote the positions where particle-plant interaction occurs. Flow is from left to right.

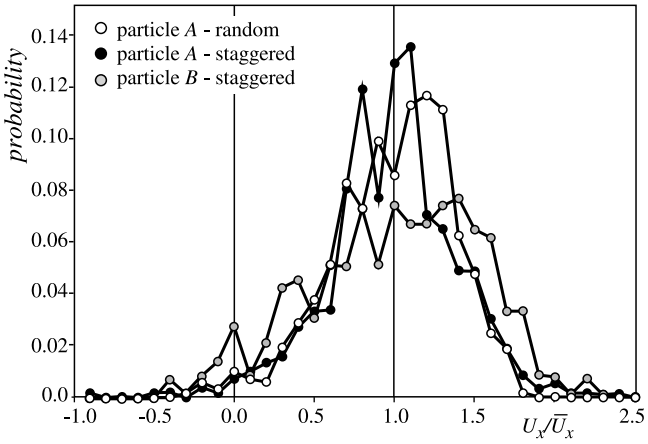

Figure 4. Probability density function of particle longitudinal velocity $U_x/\overline{U}_x$, $\overline{U}_x$ being the mean particle longitudinal velocity.

the particle is subject to an attracting force due to surface tension [*Chambert and James*, 2008].

[22] We also observe inertial impaction [*Palmer et al.*, 2004], which occurs when a particle deviates from a streamline because of its inertia and collides with a leaf. However, because the particle size is comparable to the leaf diameter, after the collision the particle goes around the leaf and, if its inertia overcomes the attractive force due to the Cheerios effect, it continues its way downstream. We specify that this mechanism can hardly be distinguished from surface tension attraction mechanism.

[23] Wake trapping [e.g., *White and Nepf*, 2003] is also observed: When a particle enters the unsteady recirculation zone behind a plant it follows an irregular path until it escapes or it is captured by a leaf through the Cheerios effect. However, in the present experiments very few particles are observed to enter the wake region behind a plant, which is consistent with the findings of *Merritt and Wohl* [2002].

[24] It is to be specified that a plant is a porous obstacle to flow and the (weak) velocity defect region behind one plant is given as the superposition of all wakes forming behind each individual leaf of the plant; these wakes create a randomly heterogeneous velocity field that contributes to particle dispersion. More intense wake regions actually form behind groups of densely arranged leaves as in Figure 3. When a particle comes close to a leaf and the attractive force due to the Cheerios effect overcomes particle inertia then the particle is captured and stays firmly attached to the leaf.

[25] Particle capture also occurs when a few leaves of one plant (or, sometimes, of two adjacent plants) weave each other to form a netlike structure that intercepts the floating particle. When a particle is captured through this mechanism, which is here referred to as net trapping, it remains finally trapped. Sometimes, a trapped particle fastened to a single leaf through the Cheerios effect is observed to escape. The escaping occurs either when the particle is stricken by an energetic turbulent event (in this case we also observe a rapid shaking of the leaf) or, more frequently, when a particle is shaken off due to the quasiperiodic vibration of the leaf it is attached to.

[26] In fact, we observe most of the leaves to vibrate at a frequency corresponding to that of vortex shedding. In the experiments the Reynolds number Re_d ($Re_d = Ud/\nu$, with d the diameter of a leaf, U the bulk flow velocity, and ν the kinematic viscosity) is in the range Re_d = 120–150 (i.e., within the regular range from the beginning of the vortex shedding at $Re_d \simeq 47$ up to the transition of the wake at $Re_d \simeq 180$). In this range we have [e.g., *Fey et al.*, 1998]

$$Sr(Re_d) = 0.2684 - \frac{1.0356}{\sqrt{Re_d}}, \tag{1}$$

where S_r is the Strouhal number ($S_r = fd/U$, with f the vortex shedding frequency). From equation (1) we have f = 5.2–6.9 Hz that well corresponds to the observed frequency at which leaves vibrate.

[27] The amplitude of leaf oscillations we observe in the present experiments is approximately a_d = 2–3 mm; therefore the maximum transverse velocity of a particle attached to a leaf is $2\pi a_d f \approx 0.13$ m/s, which is greater than the mean flow velocity. Therefore, vibrating leaves might be capable of shaking off particles by overcoming the Cheerios effect.

[28] We specify that this study considers low floating particle concentration. In fact, we observed that at moderately high particle concentration, the Cheerios effect promoted the formation of clusters comprised with a few particles. The clusters had a relatively smaller average velocity because of the more frequent interactions with the vegetation and were more easily captured by the vegetation as they get stuck against a group of few leaves.

[29] In view of the mathematical model for floating particle trapping and diffusion described in the next section, we summarize the relevant, qualitative experimental observations as follows:

[30] (1) When a particle interacts with a plant (i.e., with one leaf or a few leaves) it can be slowed down, temporarily captured, or permanently captured.

[31] (2) Mechanisms that slow down a particle are the Cheerios effect, inertial impaction, and wake trapping. Typical time delay in the particle propagation produced by this slowdown is about 2 s in the present experiments.

[32] (3) If the attractive force, between a particle and a leaf, promoted by the Cheerios effect, overcomes particle inertia, then the particle gets stuck to the leaf. However, the particle can escape thanks to the leaf vibration induced by the alternate vortex shedding. In the present experiments,

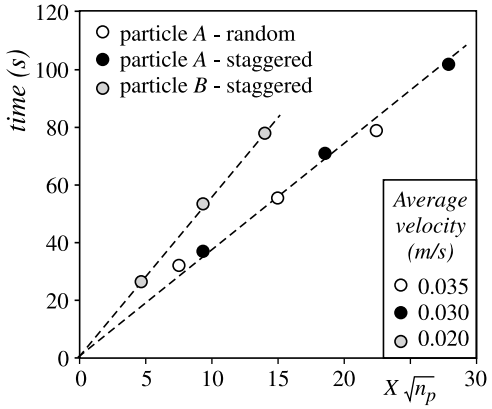

Figure 5. Mean time taken by particles to reach the fixed cross sections located at the nondimensional distances $X\sqrt{n_p}$ from the upstream end of the test section.

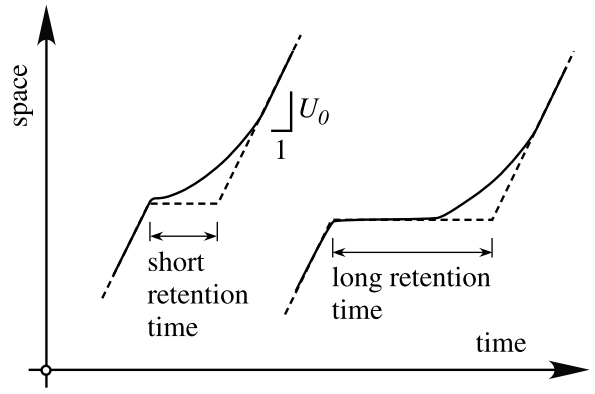

Figure 6. Actual (full line) and modelled (dashed line) world lines of a particle in the space-time diagram.

this temporary trapping event produces a time delay in the particle propagation of some tens of seconds.

[33] (4) When a particle is trapped through the net trapping mechanism or through the Cheerios effect by one leaf that cannot vibrate, the retention time is measured to be at least one order of magnitude greater than the previous one (i.e., more than 600 s in the present experiments). In this case we assume that the particle is permanently captured.

2.2. The Stochastic Model

[34] We propose a stochastic model to simulate the transport and diffusion of floating particles and the trapping mechanisms observed in the experiments. The model is one-dimensional and describes particle-vegetation interactions along the curvilinear axis s corresponding to the generic particle trajectory. The place, along s, where a particle interacts with one leaf (or a few leaves) is here referred to as interaction point. We dissect the particle path into segments Δs, Δs being the mean spacing between plants, and assume that the interaction points (one within each segment Δs) are arranged randomly in space with a uniform pdf.

[35] In the experiments we sometimes observe a particle interacting with two or more leaves of the same plant, wide apart from each other (i.e., more than one interaction process with the same plant occurs). Here we assume that the slowdown process experienced by a particle interacting with more than one leaf of the same plant can be lumped into one single interaction event.

[36] The proper specification of the length scale Δs is important to assess the model performance, as we will show. The mean center-to-center spacing between adjacent plants is $\Delta s_1 = 1/\sqrt{n_p}$, n_p being the number of plants per unit area. The mean spacing along any straight line parallel to the direction of flow, is $\Delta s_2 = 1/n_p d_p$, d_p being the diameter of the plant [*White and Nepf*, 2003].

[37] Based on comparison between model and experimental results we find that Δs_1 performs better than Δs_2; therefore the model assumes $\Delta s = 1/\sqrt{n_p}$. Let P_i be the probability that a particle interacts with a plant (i.e., with a leaf or a group of leaves) while travelling the distance Δs along its path, transported by the flow (on average, a particle interacts with one plant over a path whose length is $\Delta s/P_i$). Let P_c be the probability that a particle is permanently captured, if it interacts with a plant. Then, the probability that a particle travels a distance X greater than L before being finally captured is

$$P(X > L) = (1 - P_i P_c)^{n_L} \tag{2}$$

where n_L is the number of interaction points (i.e., plants) the particle meets within the distance L. We extend n_L to assume noninteger values and write $n_L = L/\Delta s$. Equation (2) is then rearranged to read

$$P(X > L) = e^{-L/\lambda}, \tag{3}$$

where $\lambda = -\Delta s/\ln(1 - P_i P_c)$ is the particle mean path length, while $1/\lambda$ is commonly referred to as retention coefficient [e.g., *Riis and Sand-Jensen*, 2006].

[38] In the following we consider temporary trapping processes. We denote with t_0 the average time a particle spends to travel the distance Δs if no interactions with the vegetation occur. If a particle interacts with a plant and t is the time the particle actually spends to cover the distance Δs, then we define $\tau = t - t_0$ as the retention time and we assume that a particle travels within each segment Δs with velocity $U_0 = \Delta s/t_0$ and it is temporarily arrested for the time τ (see Figure 6). Therefore, retention time, as presently defined, includes the delay due to the acceleration of a particle toward the velocity U_0. The velocity U_0 is slightly greater than the bulk velocity U both because the free surface velocity is greater than the depth average velocity and because of the channelling effect induced by plants.

[39] When a particle interacts with the vegetation, within the generic Δs, it has the probability $1 - P_c$ of being temporarily trapped. As stated at the end of section 2.1, two different interaction mechanisms are mainly responsible for particle propagation delay (i.e., particle slowdown by the Cheerios effect, inertial impaction, and wake trapping, and temporary trapping events which occur when the attractive force due to the Cheerios effect overcomes particle inertia). Accordingly, we introduce a short (subscript S) and a long (subscript L) retention time and denote with P_S the probability that a particle is trapped for a short retention time (while $P_L = 1 - P_S$ is the probability that a particle is trapped for a long retention time). The model further assumes that both short and long retention times are random and exponentially distributed with mean retention times T_S and T_L, respectively.

[40] We specify that distinguishing long retention time trapping from permanent (i.e., infinite retention time) trapping is a reasonable modeling approximation. In fact, long and infinite retention times rely on two different trapping mechanisms. However, the issue deserves further investigation.

[41] Floating particles are also subject to turbulent diffusion due to the temporal and spatial heterogeneity of the surface velocity field [e.g., *White and Nepf* 2003]. This is included in the model; however, because the heterogeneity of the velocity field is moderately weak and the distance travelled by a particle before being definitely captured is relatively short, turbulent diffusion plays a minor role in affecting the dispersion pattern.

[42] The overall model is schematically illustrated in Figure 7. An analytical expression for the particle arrival-time distribution function at prescribed cross sections is given in Appendix A. However the analytical model is hard to handle and it does not account for the turbulent diffusion. For

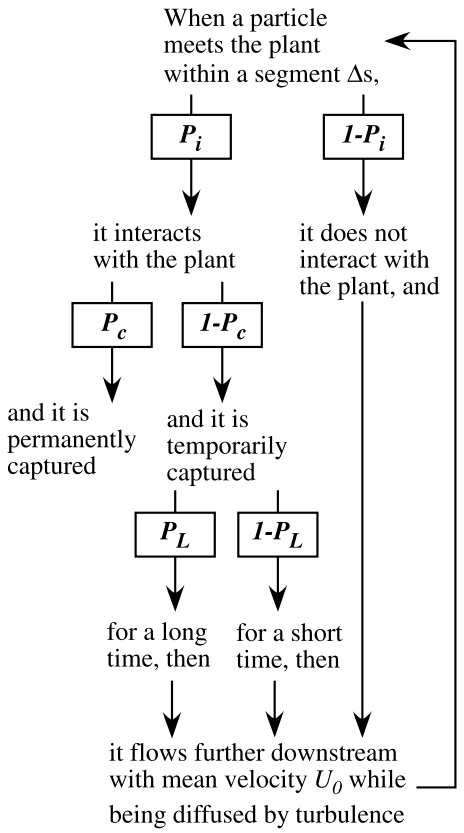

Figure 7. Schematic of the proposed model.

these reasons we also set up a random walk particle-tracking model (see Appendix B), which we checked against the analytical solution. The theoretical results presented and discussed in the next section are obtained as the ensemble average of 10000 realizations computed with the random walk model.

3. Results and Discussion

[43] Within the Lagrangian framework we measure the distance x travelled by each single particle, released just upstream of the test section, before it is permanently trapped by a plant. We can thus compare experiments with equation (3).

[44] Figure 8 shows the probability a particle has of travelling a distance X greater than L for the three investigated cases: the experimental points actually follow an exponential law. This result, which largely corresponds with results from other studies [e.g., *Riis and Sand-Jensen*, 2006], is confirmed by the Eulerian measurements where we count the number of the released particles that reach and eventually pass some fixed cross sections downstream from the beginning of the test section (Figure 8, square symbols).

[45] Particle B is more susceptible to permanent trapping than particle A, although both particles have approximately the same density, and particle B, because of its greater size, has a much larger inertia. This is because, due to its size, particle B is more frequently captured through the net trapping mechanism. In fact, particle trapping through the net trapping mechanism occurs in 65% of cases for particle B and only in 45% of cases for particle A.

[46] We determine the probability P_iP_c for each of the three different experimental conditions (see Table 1) by fitting equation (3) to the experimental data. For particle A the product P_iP_c (or, equivalently, the nondimensional retention coefficient $\Delta s/\lambda$) remains approximately the same no matter the vegetation distribution and density. We speculate that, if a particle interacts with a plant, then the probability P_c that this interaction will produce a permanent capture depends mainly on the particle and vegetation characteristics and on the flow velocity; on the contrary it is weakly affected by the vegetation distribution and density. Therefore, since P_iP_c remains approximately the same for particle A, we conclude that the probability P_i of having an interaction does not depend on the vegetation distribution and density as well.

[47] This observation can be extended to the other model parameters that describe the local particle-vegetation interaction processes. Therefore, the parameters P_L, T_L, and T_S are expected to remain the same for the two vegetation configurations that use particle A. This idea is further supported by observing that even with a regular distribution of plants (i.e., the staggered configuration), from the point of view of

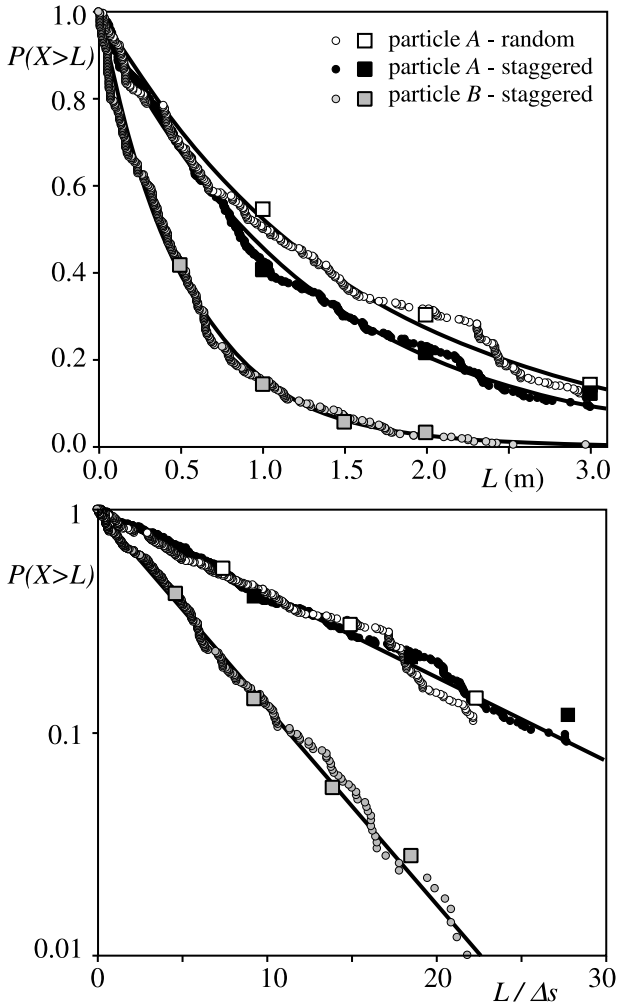

Figure 8. Experimental probability distribution $P(X > L)$ compared to equation (3). Probability is plotted versus L in the upper panel and versus $L/\Delta s$ in the lower panel. Circles and squares denote Lagrangian and Eulerian experimental results, respectively.

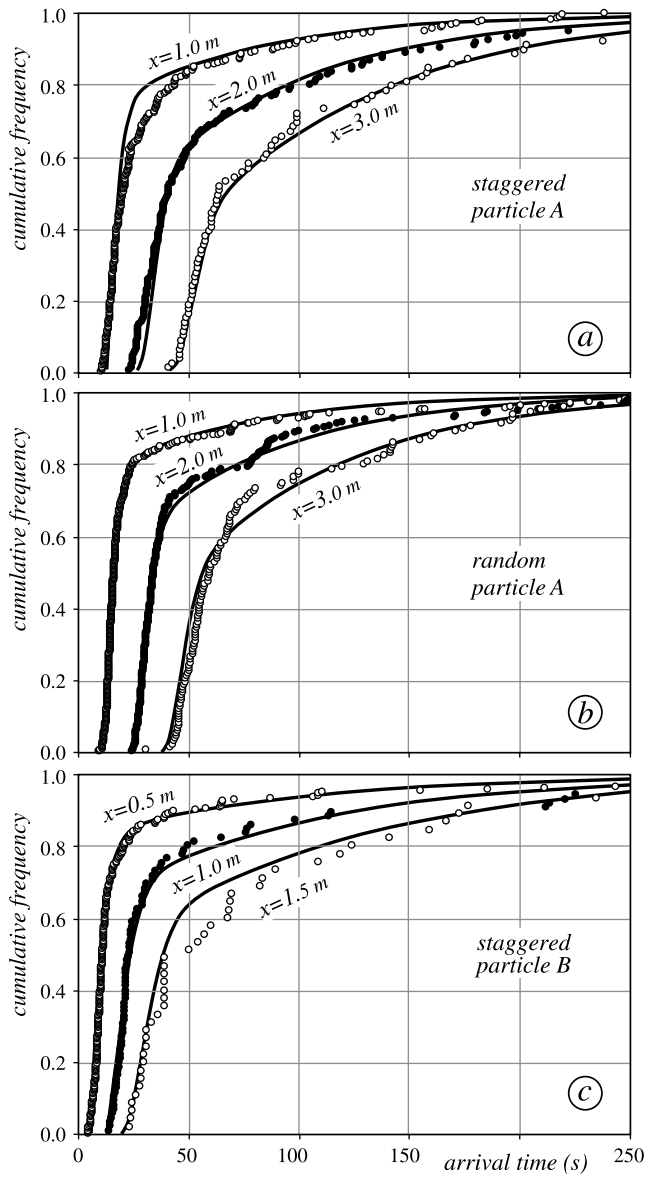

Figure 9. Cumulative arrival-time distributions: Comparison between experimental results (circles) and model predictions (full line).

a particle that is travelling along its path, interaction points appear to be randomly distributed with mean spacing Δs.

[48] Within the Eulerian framework we also measure the time spent by particles to reach (and pass) some fixed cross sections and we use these data to construct the cumulative arrival-time distributions. The experimental results are compared to the model predictions in Figure 9. The values for the model parameters used in the computations and reported in Table 1 are determined through a trial-and-error calibration procedure.

[49] In order to calibrate the model we preliminarily performed a sensitivity analysis to determine the effects of each single parameter on the arrival-time distribution. We then calibrated the model through a trial-and-error procedure and checked the possibility of forcing model parameters to have the same value for different experimental configurations (e.g., values for P_L, T_L, and T_S are the same for particle A and different vegetation configurations).

[50] Model predictions compare favorably with experimental observations. The discrepancies shown in Figure 9 can be mainly ascribed to the irregular morphology of the plants (see Figure 3). Indeed, the number of interactions experienced by each particle along its path is moderately small and the experimental paths cannot be safely regarded as realizations of a purely random process. Therefore, the experimental data used to determine the arrival-time distributions are not statistically suitable enough to unambiguously serve as a basis for a definitive comparison with the model predictions.

[51] We observe an elbow in the curves plotted in Figure 9 that reflects the two different (short and long) retention-time distributions. For particle A, the two different vegetation configurations produce rather different arrival-time distributions (Figures 9a and 9b). In particular, the elbow in the curves for the case of random distribution is significantly sharper than for the case of staggered distribution. Note that the model parameters P_i, P_c, P_L, T_S, and T_L are actually the same for both the vegetation distributions. This suggests that the observed different behaviors are solely (and effectively) controlled by the spacing Δs (i.e., the vegetation density) and that the choice of the length scale $\Delta s = 1/\sqrt{n_p}$ is reliable (see also Figure 5). In addition, this result confirms the idea that the model parameters depend on the local characteristics of the particle-vegetation interaction process and are unaffected or weakly affected by the vegetation distribution and density.

[52] For the case of staggered configuration and particle A the mean number of interactions within the 3 m long test section is $3P_i/\Delta s \approx 8$, which is consistent with the example shown in Figure 3 where the arrows denote intense particle slowdowns.

[53] Particle B, because of its greater inertia and size, is more susceptible to interact with the vegetation (it has a greater P_i) than particle A. However, the probability of being slowed down or temporarily captured (which is given by $P_i\ (1 - P_c)$) is lower for particle B than for particle A. This behavior reflects the greater inertia of particle B that, accordingly, is less affected by the attractive force between a particle and a leaf promoted by the Cheerios effect. Interestingly, the probability P_L is the same for both particles A and B. This suggests that the ratio between the number of slowdown events and temporarily trapping events might be independent from particle characteristics.

[54] Short retention time for particle B is slightly greater than that for particle A. This again reflects the greater inertia of particle B, which requires a longer time to regain the mean transport velocity once it is slowed down or arrested by one leaf.

[55] The computed arrival-time distributions plotted in Figure 9 include turbulent diffusion due to the spatially nonuniform velocity field. The order of magnitude of the longitudinal diffusion coefficient D, is estimated on the basis of the few recorded particle trajectories. We consider only trajectory segments that do not include interaction events and compute D as $D = \sigma_U^2 \Delta t/2$, σ_U being the standard deviation of the longitudinal velocity and $\Delta t = 0.08$ s is the inverse of the frame rate: we find $D \approx 2 \times 10^{-5}$ m^2/s. This is admittedly a very small diffusion coefficient that is, how-

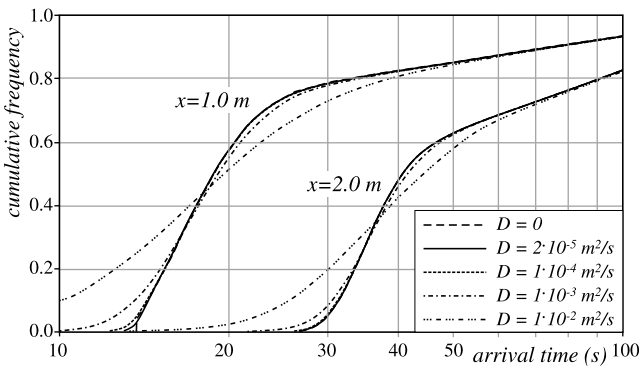

Figure 10. Cumulative arrival-time distributions computed for different values of the diffusion coefficient. Model parameters used in the computations are those for particle A and staggered distribution of plants.

ever, consistent with the small flow velocity (and Reynolds number) in the experiments.

[56] To assess the impact of turbulent diffusion we compute the arrival-time distribution for different values of the diffusion coefficient. An example of these computations is shown in Figure 10, where we see that increasing the diffusion coefficient by one or two orders of magnitude, turbulent diffusion has a minor impact on the solution. Note that the curves for $D = 0$, $D = 2 \times 10^{-5}$ m^2/s, and $D = 1 \times 10^{-4}$ m^2/s can hardly be distinguished. This result confirms that dispersion of floating particles in the presence of emergent vegetation is mainly related to particle-vegetation interaction processes.

4. Conclusions

[57] Although this study is not extensive enough to create a complete picture of particle-vegetation interaction processes (in fact, we use one plant type, one bulk velocity, and only two particle types and vegetation configurations), some preliminary conclusions can be drawn from our results, which are summarized as follows.

[58] When the flow velocity is low, as in the present experiments, floating particle dispersal is mainly governed by the random time delays in the particle propagation promoted by different particle-vegetation interaction processes; whereas turbulent diffusion, generated by the heterogeneity of the surface velocity field, plays a minor role.

[59] Distinguishing short from long retention times on the basis of the different particle-vegetation interaction mechanisms observed in the experiments, looks effective. Distinguishing long retention time from permanent trapping is indeed a reasonable modeling approximation. In fact, long and infinite retention times rely on two different trapping mechanisms. However, the issue deserves further investigation.

[60] Some of the observed particle-vegetation interaction mechanisms also deserve deeper study (e.g., the ability of leaves to shake off particles by overcoming the attractive force due to the surface tension).

[61] Indeed, a wider range of experimental conditions need to be investigated mainly to verify that the model parameters P_i, P_c, P_L, T_S, and T_L do not actually depend on the vegetation configuration and density, whose impact is only controlled by the average spacing Δs and to assess the impact of flow velocity on diffusion processes. In fact, at higher flow velocities the importance of the Cheerios effect is expected to decrease because of the greater particle inertia. In this case turbulent diffusion, which increases with flow velocity, will likely be more effective in affecting particle transport and diffusion.

Appendix A: Analytical Expression for the Arrival-Time Distribution Function

[62] We focus on particles that actually travel the distance $X \geq L$ (i.e., particles that are permanently captured over a path shorter than L are a priori excluded from the present analysis), and we assume that the number of interaction points, $n = L/\Delta s$ within the distance L is an integer.

[63] The probability $p(k)$ that a particle interacts k (of n) times with the vegetation has a binomial distribution with mean nP_i and variance $nP_i(1 - P_i)$

$$p(k) = \frac{n!}{k!(n-k)!} P_i^k (1 - P_i)^{n-k}, \tag{A1}$$

P_i being the probability that, at each interaction point, the particle actually interacts with the vegetation.

[64] When a particle interacts with one leaf it can be either slowed down (i.e., trapped for a short time, see Figure 6) or trapped for a long time (as stated above, permanent trapping is not considered here).

[65] Let m ($\leq k$) be the number of short-time trapping events. The probability of having m out of k short-time interactions follows a binomial distribution

$$q(m) = \frac{k!}{m!(k-m)!} P_S^m (1 - P_S)^{k-m}, \tag{A2}$$

where P_S s the probability that the interaction event is actually a short-time interaction.

[66] The retention-time distribution $r_{m,k}(t)$, for a particle that experiences m short-retention-time trapping events out of k (temporarily) trapping events is then given as

$$r_{m,k}(t) = \underbrace{p_S * p_S * \ldots * p_S}_{m \text{ times}} * \underbrace{p_L * \ldots * p_L}_{k-m \text{ times}}, \tag{A3}$$

where $*$ denotes convolution and

$$p_S(t) = \frac{1}{T_S} e^{-t/T_S}, \; p_L(t) = \frac{1}{T_L} e^{-t/T_L}, \tag{A4}$$

are the short- and long-retention-time distributions, here assumed to be exponential with means T_S and T_L, respectively.

[67] The retention-time distribution is then given as

$$r(t) = \sum_{k=0}^{n} \left[p(k) \sum_{m=0}^{k} q(m) r_{m,k}(t) \right]. \tag{A5}$$

[68] Equation (A5) gives the time a particle spends at rest (in the sense of the proposed model; see Figure 6). To determine the total time a particle spends within the reach L

we must add the particle travel time which is affected by the turbulent diffusion mainly due to the spatially nonuniform velocity field. Assuming a Fickian diffusion, the travel-time distribution $h(t)$ is then given as

$$h(t) = \frac{L}{4\sqrt{\pi D t^3}} e^{-\frac{(L-U_0 t)^2}{4Dt}}, \tag{A6}$$

where D is the diffusion coefficient.

[69] The arrival-time distribution function $a(L,t)$ is then given as the convolution of equations (A5) and (A6)

$$a(L,t) = \sum_{k=0}^{n} \left[p(k) \sum_{m=0}^{k} q(m) \left(r_{m,k}(t) * h(t) \right) \right]. \tag{A7}$$

[70] If we neglect diffusion, then $h(t)$ reduces to the Dirac Delta function $\delta(t - t_0)$, with $t_0 = L/U_0$, and equation (A7) can be rewritten as

$$a(L,t) = \begin{cases} 0 & t \le t_0 \\ \sum_{k=0}^{n} \left[p(k) \sum_{m=0}^{k} q(m) r_{m,k}(t - t_0) \right] & t > t_0 \end{cases}, \tag{A8}$$

where $p(k)$ and $q(m)$ are given by equations (A1) and (A2) respectively, and the retention-time distribution $r_{m,k}(t)$ can be developed as follows.

[71] By combining equations (A3) and (A4), we find that $r_{m,k}(t)$ is given as the convolution between two Gamma distributions associated with the short and the long retention times respectively

$$r_{m,k}(t) = \left[\frac{t^{m-1} e^{-t/T_S}}{T_S^m (m-1)!} \right] * \left[\frac{t^{k-m-1} e^{-t/T_L}}{T_L^{k-m} (k-m-1)!} \right]. \tag{A9}$$

[72] Equation (A9) is expanded to read

$$r_{m,k}(t) = \frac{e^{-t/T_L}}{T_S^m T_L^{k-m} (m-1)!(k-m-1)!} \times \int_0^t e^{\Psi\tau} \tau^{m-1} (t-\tau)^{k-m-1} d\tau, \tag{A10}$$

where $\Psi = 1/T_L - 1/T_S$. Equation (A10) is then recast as

$$r_{m,k}(t) = \frac{e^{-t/T_L} t^{k-1}}{T_S^m T_L^{k-m} (m-1)!(k-m-1)!} \times \int_0^1 e^{\Psi t\xi} \xi^{m-1} (1-\xi)^{k-m-1} d\xi. \tag{A11}$$

[73] Recalling that

$$(1-\xi)^n = \sum_{i=0}^{n} \frac{n!}{(n-i)!i!} (-\xi)^i, \tag{A12}$$

the integral in equation (A11) can be written as

$$\int_0^1 e^{\Psi t\xi} \xi^{m-1} (1-\xi)^{k-m-1} d\xi = \sum_{i=0}^{k-m-1} \frac{(k-m-1)!}{(k-m-i-1)!i!} \cdot (-\xi)^i \int_0^1 e^{\Psi t\xi} \xi^{i+m-1} d\xi \tag{A13}$$

[74] Finally, using the following recursive formula

$$\int_0^1 e^{\Psi t\xi} \xi^n d\xi = \frac{e^{\Psi t}}{\Psi t} - \frac{n+1}{\Psi t} \int_0^1 e^{\Psi t\xi} \xi^{n-1} d\xi, \tag{A14}$$

equation (A11) is rewritten as

$$r_{m,k}(t) = \frac{e^{-t/T_L} t^{k-1}}{T_S^m T_L^{k-m} (m-1)!} \times \sum_{i=0}^{k-m-1} \frac{(i+m-1)!}{(k-m-i-1)!i!} \times \left[\frac{(-1)^m}{(\Psi t)^{i+m}} + \frac{e^{\Psi t}}{\Psi t} \sum_{j=0}^{i-m-1} \frac{(-1)^{i+j}}{(\Psi t)^j (i+m-j-1)!} \right]. \tag{A15}$$

[75] If the ratio $L/\Delta s$ is not an integer, we have $L_0 < L < L_1$, with $L_0 = n\Delta s$ and $L_1 = (n+1)\Delta s$. Because the interaction points are assumed uniformly distributed, then the arrival-time distribution is given as the following weighted average

$$a(L,t) = w a(L_0,t) + (1-w) a(L_1,t) \tag{A16}$$

with $w = (L_1 - L)/\Delta s$.

Appendix B: The Random Walk Particle-Tracking Model

[76] The random walk particle-tracking model developed to predict floating particle paths in the presence of emergent vegetation is based on the scheme shown in Figure 7. The Lagrangian trajectory of each single particle is computed using the following steps.

[77] As a first step, the model generates a series of interaction points, randomly distributed with a uniform *pdf* and one point within each segment Δs. The model then computes the particle path advancing in time by small time steps $\Delta t = 0.001$ s.

[78] At each time step the model checks if the particle has reached an interaction point. If this is not the case, the particle is advanced with velocity $U_0 + \Delta U$, ΔU being a (random) velocity fluctuation which accounts for turbulent diffusion. This velocity fluctuation is randomly generated from a Gaussian distribution with zero mean and standard deviation $\sigma_U = \sqrt{2D/\Delta t}$, D being the turbulent diffusion coefficient.

[79] When the particle reaches an interaction point a random number r is generated (with $0 \le r \le 1$, and a uniform *pdf*): if $r > P_i$ then the model assumes that the particle does not interact with the vegetation and it is advanced one time step as described above.

[80] Otherwise ($r \le P_i$), the particle is assumed to interact with the vegetation. In this case a further random number r is generated, and if $r \le P_c$, then the model assumes that the particle is permanently captured by the vegetation and the path reconstruction ends.

[81] If the particle is temporarily captured (i.e., $r > P_c$), a further random number r is generated to establish whether the temporary capture is a short-time or a long-time trapping event. If $r \le P_L$ the model assumes the interaction to be a long-time trapping event, a random retention time t_R, exponentially distributed with mean T_L is then generated and the particle is left in place for this period of time. On the contrary (i.e., if $r > P_L$) the model assumes the interaction to be a short-time interaction event; in this case a random retention time t_R, exponentially distributed with mean T_S is

generated and the particle is left in place for this period of time.

[82] The path reconstruction keeps going until the particle is permanently captured or until the particle has travelled a distance greater than or equal to the test section length. For each reconstructed path (realization) the model then gives the particle position at each time $t_i = i\Delta t$.

[83] **Acknowledgments.** We wish to acknowledge Simone Sponga and Daniele Destro for their contribution to the experimental investigations.

References

Andersson, E., C. Nilsson, and M. E Johansson (2000), Plant dispersal in boreal rivers and its relation to the diversity of riparian flora, *J. Biogeogr.*, *27*, 1095–1106.

Chambert, S., and C. S. James (2008), Sorting of seeds by hydrochory, *River Res. Appl.*, *25*, 48–61, doi:10.1002/rra.1093.

Fey, U., M. Konig, and H. Eckelmann (1998), A new Strouhal-Reynolds-number relationship for the circular cylinder in the range $47 < Re < 2 \times 10^5$, *Phys. Fluids*, *10*(7), 1547–1549.

Groves, J. H., D. G. Williams, P. Caley, R. H. Norris, and G. Caitcheon (2009), Modeling of floating seed dispersal in a fluvial environment, *River. Res. Applic.*, *25*, 582–592.

Huiskes, A. H. L., B. P. Koutstall, P. M. J. Herman, W. G. Beeftink, M. M. Markusse, and W. De Munck (1995), Seed dispersal of halophyte in tidal salt marshes, *J. Ecol.*, *83*, 559–567.

Lightbody, A. F., and H. M. Nepf (2006), Prediction of velocity profiles and longitudinal dispersion in emergent salt marsh vegetation, *Limnol. Oceanogr.*, *51*(1), 218–228.

Lopez, F., and M. Garcia (1998), Open-channel flow through simulated vegetation: Suspended sediment transport modelling, *Water Resour. Res.*, *34*(9), 2341–2352.

Merritt, D. M., and E. E. Wohl (2002), Processes governing hydrochory along rivers: Hydraulics, hydrology, and dispersal phenology, *Ecol. Appl.*, *12*, 1071–1087.

Murphy, E., M. Ghisalberti, and H. Nepf (2007), Model and laboratory study of dispersion in flows with submerged vegetation, *Water Resour. Res.*, *43*, W05438, doi:10.1029/2006WR005229.

Nepf, H. M. (1999) Drag, turbulence, and diffusion in flow through emergent vegetation, *Water Resour. Res.*, *35*(2), 479–489.

Nepf, H., M. Ghisalberti, B. White, and E. Murphy (2007), Retention time and dispersion associated with submerged aquatic canopies, *Water Resour. Res.*, *43*, W04422, doi:10.1029/2006WR005362.

Nilsson, C., and M. Danvind (1997), Seed floating ability and distribution of alpine plants along a northern Swedish river, *J. Veg. Sci.*, *8*, 271–276.

Palmer, M. R., H. M. Nepf, and T. J. R. Pettersson (2004), Observations of particle capture on a cylindrical collector: Implications for particle accumulation and removal in aquatic systems, *Limnol. Oceanogr.*, *49*(1), 76–85.

Rand, T. A. (2000), Seed dispersal, habitat suitability and the distribution of halophytes across a salt marsh tidal gradient, *J. Ecol.*, *88*, 608–621.

Riis, T., and K. Sand-Jensen (2006), Dispersal of plant fragments in small streams, *Freshwater Biol.*, *51*, 274–286.

Sharpe, R. G., and C. S. James (2006), Deposition of sediment from suspension in emergent vegetation, *Water SA*, *32*(2), 211–218.

Van den Broek, T., R. Van Diggelen, and R. Bobbink (2005), Variation in seed buoyancy of species in wetland ecosystems with different flooding dynamics, *J. Veg. Sci.*, *16*(5), 579–586.

Vella, D., and L. Mahadeven (2005), The "Cheerios effect," *Am. J. Phys.*, *73*(9), 817–825.

White, B. L., and H. M. Nepf (2003), Scalar transport in random cylinder arrays at moderate Reynolds number, *J. Fluid Mech.*, *487*, 43–79.

Wolters, M., A. Garbutt, R. M. Bekker, J. P. Bakker, and P. D. Carey (2008), Restoration of salt-marsh vegetation in relation to site suitability, species pool and dispersal traits, *J. Appl. Ecol.*, *45*, 904–912.

A. Defina and P. Peruzzo, Dipartimento di Ingegneria Idraulica, Marittima Ambientale e Geotecnica, Università di Padova, via Loredan 20, I-35131 Padua, Italy. (defina@idra.unipd.it)